Original article

Nuclear Medicine Communications

Cardiac atrial metabolism quantitative assessment with analog and digital time of flight-PET/computed tomography

Michel Hesse[a], Sébastien Marchandise[b], Bernhard Gerber[b] and Véronique Roelants[a]

Background Evaluation of left atrium (LA) remodeling is becoming increasingly relevant in understanding several pathological cardiac conditions. ^{18}F-FDG-PET/computed tomography (CT), the current gold standard for metabolic evaluation of the left ventricle, could be extended to LA using the latest PET technologies. We sought to perform a phantom study to optimize the reconstruction algorithm in this context.

Methods The liver, heart cavity and walls of an anthropomorphic phantom were filled with typical patient ^{18}F-FDG activity concentrations. Acquisitions were performed on an analog and on a digital TOF-PET/CT, and reconstructed with and without resolution recovery (RR). The Richardson-Lucy RR method was used, either through a third-party software or through the PET/CT manufacturer algorithm. Activity recoveries in the atria and ventricles and signal-to-noise ratios were evaluated to identify the best reconstruction and RR parameters. The same methodology was applied on a patient cardiac study.

Results Analog PET/CT with the third-party RR cannot improve the activity recovery without markedly degrading the image quality. For the digital PET/CT, the optimal algorithm was the manufacturer RR reconstruction using four iterations and 15 subsets combined with five RR iterations. This reconstruction improved the LA activity recovery from 58% to 70% while preserving images of diagnostic quality. Similar results were obtained for the patient study.

Conclusion The digital TOF-PET/CT with the identified optimal reconstruction can be used to quantitatively analyze the LA uptake in ^{18}F-FDG cardiac studies while still preserving image reading quality. This may lead to more precise cardiovascular disease status evaluation, especially when atria are concerned. *Nucl Med Commun* XXX: XXXX–XXXX Copyright © 2023 Wolters Kluwer Health, Inc. All rights reserved.

Nuclear Medicine Communications XXX, **XXX**:XXXX–XXXX

Keywords: atria, cardiac study, quantitation, TOF-PET/CT

[a]Nuclear Medicine Department, Cliniques Universitaires Saint-Luc and [b]Cardiology Department, Cliniques Universitaires Saint-Luc, Brussels, Belgium

Correspondence to Michel Hesse, PhD, Service de médecine Nucléaire, Cliniques Universitaires Saint-Luc, 10 avenue Hippocrate, 1200 Brussels, Belgium
Tel: +32 2 7642592; fax: +32 2 7645408; e-mail: michel.hesse@uclouvain.be

Received 24 August 2022 **Accepted** 20 March 2023.

Background

The prognostic value of the left atrium (LA) remodeling as a biomarker of outcome in several cardiovascular diseases, such as atrial fibrillation or heart failure with preserved ejection fraction, is becoming increasingly recognized [1]. Echocardiography, cardiac magnetic resonance or cardiac computed tomography have emerged as interesting noninvasive imaging techniques able to evaluate left atrial remodeling in response to electrical, mechanical or metabolic stressors [2,3]. On the other hand, LA remodeling can also be characterized from his metabolic changes observed by ^{18}F-FDG imaging with PET/computed tomography (CT) [4–6]. In fact, this modality is currently the gold standard for metabolic evaluation of the left ventricle and recently, it has been suggested that, despite the thinness of the LA wall, LA metabolism evaluation is also feasible using the latest PET camera technologies [7,8].

The last decade has seen the development of PET/CT systems along two axes that led to improvement of the spatial resolution. The first one is the improvement of the timing resolution from about 650 ps in the first time of flight (TOF)-PET/CT commercialized by Philips [9] to about 300 ps and even less in the last TOF-PET generations [10–12] (partially thanks to the use of digital SiPM detectors). The second one is the improvement of dedicated reconstruction algorithms using TOF and point spread function (PSF) information [10–13].

Consequently, in prelude to the prospective study TRIATLON (EudraCT number 2019-001813-17), the purpose of this cardiac phantom study was twofold: first, to compare images quality and uptake quantification obtained on an analog (first generation) and on a digital (last generation) LYSO TOF-PET/CT and, secondly, to determine the most appropriate advanced TOF+PSF reconstruction algorithm to quantify the LA uptake. The methodology was also evaluated clinically on one patient imaged with ^{18}F-FDG on both PET systems.

0143-3636 Copyright © 2023 Wolters Kluwer Health, Inc. All rights reserved. DOI: 10.1097/MNM.0000000000001694

Materials and methods

Phantoms

An anthropomorphic Heart/thorax phantom (Radiology Support Devices, Inc, Long Beach, California, USA) was used, whose liver, heart cavity and walls were filled with typical ^{18}F-FDG activity concentrations observed in patient studies, that is, 5, 3.8 and 15 kBq/ml, respectively. The heart part of the phantom has only two fillable regions: the cavities (about 284 ml) and the walls (about 183 ml excluding the defects volumes). It also includes two unremovable defects of about 14 and 42 ml within the walls. The defect located in the interventricular septum (42 ml) was filled with the same ^{18}F-FDG concentration as the heart walls, while the defect in the lateral wall of the left ventricle (14 ml) was only filled with water.

Single-bed position acquisitions of 10 min were performed, first using the analog camera (Philips Gemini TF64 TOF-PET/CT; Philips Healthcare, Cleveland, Ohio, USA), 620 ps TOF full width at half maximum (FWHM) and 18 cm axial FOV, and then, immediately after, using the digital one (Philips Vereos TOF-PET/CT; Philips Healthcare), 310 ps TOF FWHM and 16.4 cm axial FOV.

Reconstruction

List file data were reconstructed with a 2 mm voxel size using manufacturer ordered subset expectation maximization (OSEM) algorithms with different numbers of iterations and subsets without and with resolution recovery (RR). Images were first reconstructed using OSEM algorithms with the recommended manufacturer parameters, that is, three iterations and 33 subsets for the analog camera and two iterations and 15 subsets for the digital camera, respectively. As only the digital PET/CT includes a manufacturer PSF RR correction based on the Richardson-Lucy method, a post-reconstruction PSF RR based on the same technique, implemented as a plug-in of the open source ImageJ software (U.S. National Institutes of Health, Bethesda, Maryland, USA) [14,15], was also tested on the reconstructed images of both TOF-PET/CT.

The ImageJ RR plug-in DeconvolutionLab2 includes several deconvolution algorithms [15]. We selected the one based on the Richardson-Lucy method that has two input parameters: the PSF FWHM that we measured for both PET systems using a ^{18}F point source set at the FOV center, and an iteration number whose default value of 10 was used. In contrary, the manufacturer RR method includes a spatially variant PSF library and has two input parameters: a RR iteration number and a regularization factor [13]. For the digital PET, in addition to the manufacturer reconstruction without RR, we performed three reconstructions with the PSF RR method by setting the RR iteration parameter equal to 1, 5 and 10. The regularization parameter was not changed and was equal to six in all cases.

Activity recovery assessment

Due to the low dose CT scan, as routinely used for patients, jointly with the close Hounsfield unit values of plexiglass and water, automatic drawing of the volumes of interest (VOIs) based on a threshold was not possible. So VOIs were manually drawn around the right (RA) and left atria (LA) and ventricles (RLV) on the CT image. Measured ^{18}F-FDG activity concentrations in the atria and ventricles walls were compared to exact values to assess the activity recovery.

These CT VOIs were applied on the PET images to assess the walls activity, whatever the PET reconstruction setup (no adaptation of the VOIs to the PET activity was performed) to avoid the introduction of bias in the quantitative comparison between reconstructions with and without RR.

Signal-to-noise ratio assessment

To evaluate and compare the image quality of the PET images, signal-to-noise ratio (SNR) values were measured from a VOI obtained by using a 9 kBq/ml threshold, that is, the mean activity concentration of the heart cavity and walls, on the PET original image, that is, without RR, resulting in a volume including both the atria and ventricles walls. The SNR was calculated by dividing the VOI mean value by its SD.

Patient

To validate the phantom results, one patient of the ongoing prospective study TRIATLON (EudraCT number 2019-001813-17) was acquired on both TOF-PET/CT, and these data were analyzed similarly to the phantom data. The TRIATLON study was approved by the Institutional Ethics Committee of Brussels Cliniques Universitaires Saint-Luc, and all patients provided written informed consent.

Single-bed position acquisition of 10 min was performed on the Vereos 90 min after intravenous injection of about 296 MBq of ^{18}F-FDG, then repeated directly after on the Gemini. Acquisitions were non-gated and reconstructed with a 2 mm voxel size using three iterations and 33 subsets for the Gemini and four iterations and 15 subsets for the Vereos acquisition, respectively.

As for the actual patient uptake is unknown, the activity recovery and SNR assessments were replaced by the SUV mean and SD measurements of the VOI.

Results

Phantoms

The PET images of the anthropomorphic phantom acquired on the analog and on the digital PET/CT are depicted in Fig. 1. The reconstructions without

Fig. 1

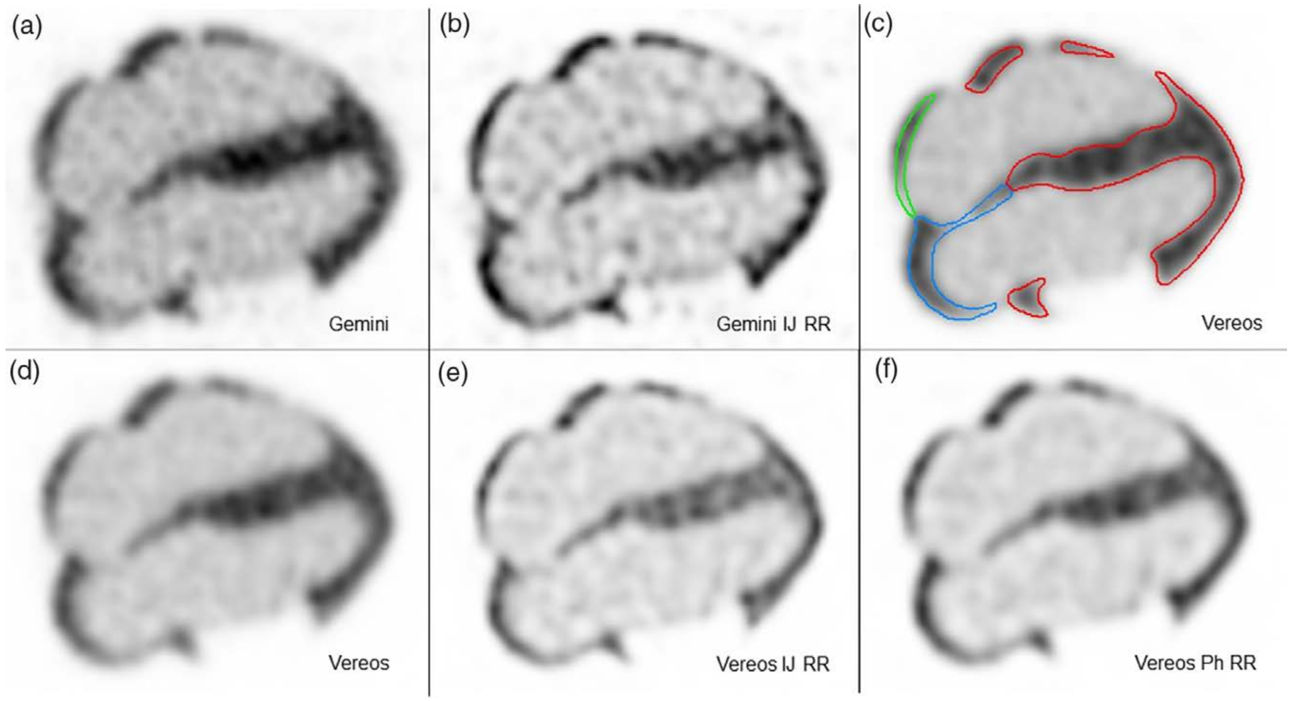

PET reconstructions of the heart insert of the anthropomorphic phantom. (a and b) Gemini system; (d, e, and f) Vereos system. (a and d) Manufacturer reconstructions without RR; (b and e) manufacturer reconstructions with ImageJ (IJ) RR; (f) manufacturer reconstruction including Philips (Ph) RR with 5 iterations/6 regularization; (c) manually drawn VOIs around the left atrium (blue), the right atrium (green) and the ventricles (red) shown on the Vereos image. RR, resolution recovery.

RR already clearly show the better image quality (less noise and better delineation of the walls) provided by the digital TOF-PET/CT (Fig. 1d) versus the analog one (Fig. 1a) due to its improved physical characteristics [10,11]. As expected from deconvolution techniques [16], such as the ImageJ plug-in Richardson-Lucy method [14,15] (Fig. 1b and 1E), the spatial resolution improvement (characterized by the appearance of a thinner wall) is accompanied by an image noise increase, especially in the case of the analog PET/CT (Fig. 1b). For the digital PET/CT (Fig. 1f), the manufacturer reconstruction RR algorithm which includes the spatially variant PSF, appears to provide, in five iterations, a spatial resolution as good as the ImageJ RR method together with a less noisy image appearance.

As seen in Fig. 2, VOIs were manually drawn around the right and left atria and around the ventricles walls of the cardiac phantom. The defect located in the lateral wall of the left ventricle and the remaining air bubbles in the phantom walls were excluded from the VOIs.

As we are looking for the best imaging technique for atrial uptake evaluation, we optimized the reconstruction parameters only for the images obtained with the Vereos digital TOF-PET/CT. The convergence of the LA activity recovery as a function of the reconstruction iteration number is displayed in Fig. 3a. Similar curves are obtained for the RA and RLV activity recoveries with slightly different absolute values (data not shown). For all reconstructions, the convergence of the activity recovery is reached at a product between iterations and subsets of 60. The maximum LA activity recovery increases from about 58% without RR to about 74% with a 10 iterations RR.

Figure 3b shows that the SNR in the digital PET final image is impacted by both the reconstruction and the RR iteration numbers.

We choose as best reconstruction parameters, 4 iterations × 15 subsets for the OSEM algorithm and 5 iterations for the manufacturer RR algorithm (we will later discuss this choice).

Table 1 illustrates the quantitative impact of the RR correction on the activity recoveries in the right and left atria and ventricles walls and on the image quality for both TOF-PET/CT. Standard reconstruction parameters were used for the Gemini while optimum values were selected for the Vereos. As seen in Fig. 1, using a RR method leads to an improved spatial resolution, and as a consequence to an improved activity recovery, whatever the TOF-PET/CT considered.

Fig. 2

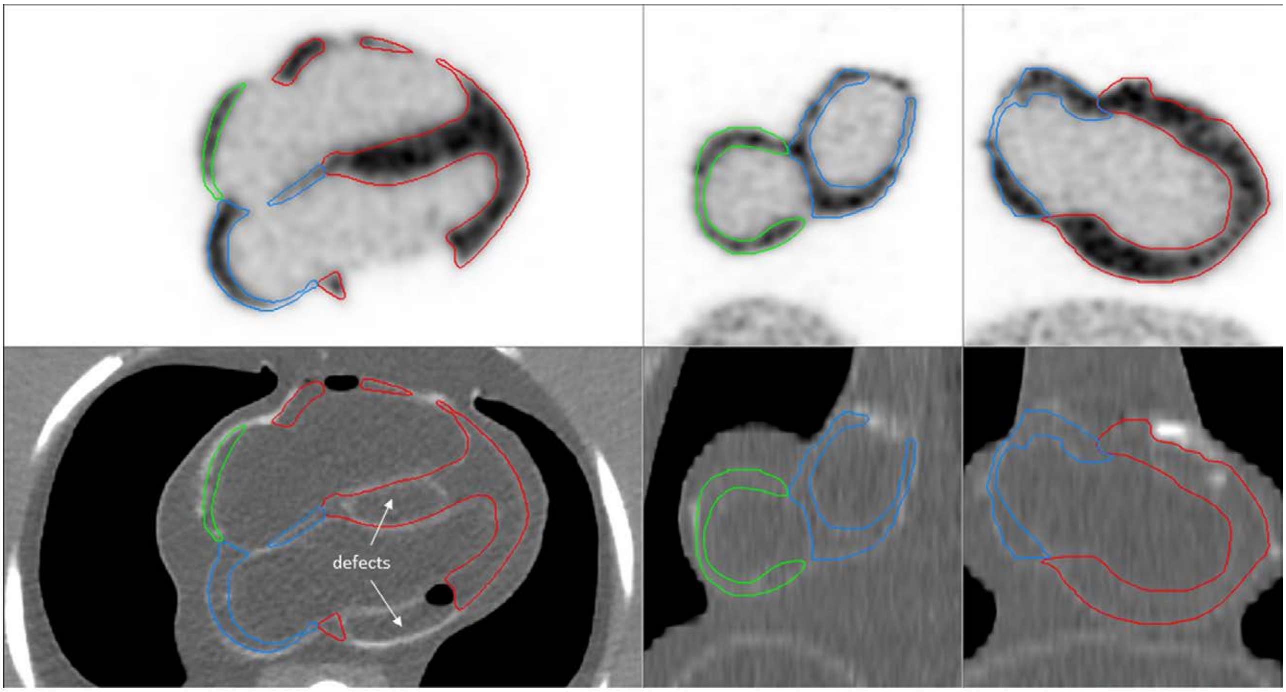

PET (top row) and CT (bottom row) images of the phantom from the Vereos with VOIs drawn around the left atrium in blue, the right atrium in green and the ventricles walls in red, respectively. Regarding the two defect inserts of the phantom, the upper one was filled with the same ^{18}F-FDG concentration as the heart walls, while the other one was only filled with water. CT, computed tomography.

Fig. 3

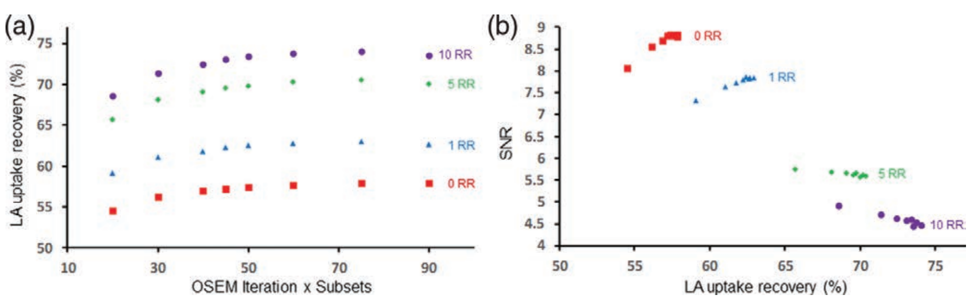

(a) Activity recovery values for the LA wall as a function of the iteration number of the OSEM reconstruction for the Vereos acquisition. (b) SNR value with respect to the LA wall activity recovery. Red squares correspond to the reconstruction without RR (0 RR). Blue triangles, green diamonds and purple circle dots correspond to the reconstruction with the manufacturer RR using 1, 5 and 10 RR iterations, respectively. RR, resolution recovery; SNR, signal-to-noise ratio.

However, the SNR, quantifying the image quality, is already worse in the analog PET image without RR and drops strongly after applying the ImageJ RR. Using the selected optimum set of manufacturer RR reconstruction parameters for the digital TOF-PET/CT provides improved activity recoveries of about 70% for the atria and 80% for the ventricles, that is, about the same as the ImageJ RR method, but with a drop of only 37% of the SNR versus 43% with the ImageJ RR.

Patient

Figure 4 compares the PET images of one patient ^{18}F-FDG cardiac studies on the Gemini and Vereos TOF-PET/CT and reconstructed using OSEM algorithms with the standard three iterations and 33 subsets for the Gemini and the optimized four iterations and 15 subsets for the Vereos, respectively. Like for the phantom images, the Vereos reconstruction without RR is clearly superior to the Gemini one, as can be seen from the hardly visible left atrium wall and interatrial septum on

Table 1 Activity recoveries for the right and left atria and ventricles walls together with the SNR for the manufacturer reconstructions on the Gemini and Vereos TOF-PET/CT, without RR, with ImageJ RR and, for the Vereos, with the Philips RR

		Activity recoveries (%)			
TOF-PET/CT	Reconstruction	Left atrium	Right atrium	Ventricles	SNR
Gemini	Without RR	60	63	74	6.8
3 it × 33 subs	With ImageJ RR	73	71	81	3.9
Vereos	Without RR	58	57	72	8.9
4 it × 15 subs	With ImageJ RR	68	66	78	5.1
	With 5 it Philips RR	70	71	80	5.6

RR, resolution recovery; SNR, signal-to-noise ratio; TOF-PET/CT, time of flight-PET/computed tomography.

Fig. 4

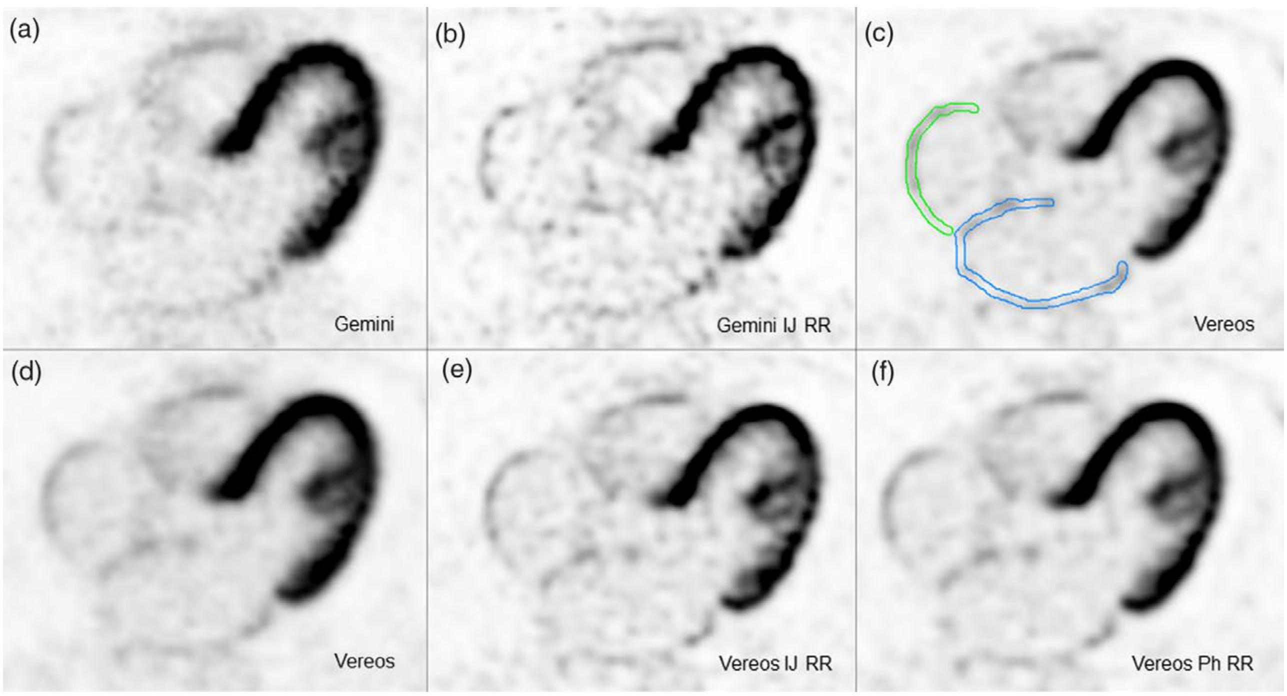

PET reconstructions of a patient ^{18}F-FDG cardiac study. (a and b) Gemini system; (d, e, and f) Vereos system. (a and d) Manufacturer reconstructions; (b and e) manufacturer reconstructions with ImageJ (IJ) RR; (f) optimized manufacturer reconstruction including Philips (Ph) RR with 5 iterations/6 regularization; (c) manually drawn VOIs around the right (in green) and left (in blue) atria shown on the standard Vereos image. RR, resolution recovery.

Table 2 SUV mean and SD values for the right and left atria and left ventricle walls of a patient cardiac study for the manufacturer reconstructions on the Gemini and Vereos TOF-PET/CT, without RR, with ImageJ RR and, for the Vereos, with the Philips RR

		Left atrium		Right atrium		Left ventricle	
TOF-PET/CT	Reconstruction	Mean SUV	SD SUV	Mean SUV	SD SUV	Mean SUV	SD SUV
Gemini	Without RR	2.16	0.87	1.95	0.54	11.84	2.92
3 it × 33 subs	With ImageJ RR	2.26	1.45	2.33	1.01	13.49	4.52
Vereos	Without RR	2.13	0.64	2.10	0.59	11.27	2.49
4 it × 15 subs	With ImageJ RR	2.24	1.03	2.37	0.93	12.59	3.68
	With 5 it Philips RR	2.44	0.99	2.50	0.90	13.84	3.71

RR, resolution recovery; TOF-PET/CT, time of flight-PET/computed tomography.

the Gemini image (Fig. 4a). On the Vereos images, the atria walls become better defined after RR, with the manufacturer spatially variant PSF method providing the best results in terms of image quality (Fig. 4f).

Table 2 provides a quantitative analysis of the patient cardiac PET reconstructions. The RR increases the mean SUV but also the SD, as expected from the phantom results (Table 1). Like for the heart phantom, the manufacturer spatially variant PSF RR reconstruction available on the Vereos TOF-PET/CT provides the best compromise between the atria uptake improvement and the noise level increase, that is, highest mean SUV associated with SD values similar to the ImageJ RR.

Discussion

To the best of our knowledge, it is the first time that a phantom study is performed to identify the best reconstruction algorithm to compare the LA uptake in patient ^{18}F-FDG cardiac studies between analog and digital TOF-PET/CT. As the analog TOF-PET/CT system does not include any RR option in the reconstruction algorithm, a third-party post-reconstruction RR based on the Richardson-Lucy method was considered (ImageJ DeconvolutionLab2 plug-in).

While this third-party post-reconstruction RR method clearly improves the spatial resolution and cardiac walls activity recoveries by using a constant PSF (Fig. 1 and Table 1), it is not optimized to the PET image specificities like the manufacturer algorithm that includes a RR that takes into account the PSF variations according to the location in the field of view [13]. This results in noisier images, especially in the case of the analog TOF-PET/CT whose original reconstruction is already more impacted by noise (Fig. 1). Noisier images will result in less reliable activity measurements as they are very sensitive to the VOIs drawing.

Figure 3b shows, for the Vereos TOF-PET/CT, that when no RR or a light RR (only one iteration) is performed, the SNR behaves like an increasing function of the LA activity recovery, while for higher RR iteration numbers, it becomes a decreasing function. This induces that a compromise has to be made between the LA activity recovery and the image reading quality. A post filtering of the image is still possible to make a noisier image more readable. However, one should be careful when pushing the RR algorithms too far (disregarding the SNR) as one might end up with artefactual images that are no more representative of the activity distribution, typically by producing edge artifacts [17,18].

Based on the evaluation of the image quality by our nuclear medicine physicians, we selected as best OSEM reconstruction parameters the values of four iterations and 15 subsets as these values correspond to the beginning of the convergence plateau of the activity recovery (Fig. 3a), and higher values lead to noisier images. For the manufacturer RR parameter we decided to limit the number of iterations to five as the SNR drops quite fast for higher values (Fig. 3b). In this study, we did not play with the regularization parameter of the manufacturer RR algorithm that was fixed to the recommended value of six. Optimizing this parameter, whose function is to drive the image smoothness, might still improve the image quality by reducing the noise level but we do not expect it to alter much the optimized set of parameters found in this quantitative study. Together these parameters provide a LA activity recovery of about 70%.

The ^{18}F-FDG cardiac studies performed on both TOF-PET/CT with the same patient confirmed the results obtained with the phantom. Compared to the phantom the patient heart was about 10% larger, but ventricular and atrial wall thicknesses were very similar, with values measured on MRI between 0.9 and 1.5 cm for the LV and between 1 and 3 mm for the LA. The atria uptake in clinical studies can be much lower than values observed with the phantom (Figs. 1 and 4) because the heart phantom includes only one volume for ventricles and atria walls. However this has no impact on the best recovery parameters as these depend only on the PET spatial resolution. The limited spatial resolution of the Gemini PET makes it unfit to study the atria metabolism as the atria walls and interatrial septum are hardly seen on the reconstructed images (Fig. 4). On the other hand, these structures are already visible on the Vereos reconstruction without RR and become sharper when using a RR algorithm. The manufacturer reconstruction including the PSF RR still provide a better image quality compared to the post-reconstruction RR (Fig. 4 and Table 2).

Unlike the cardiac phantom filled in the present study with a homogeneous activity distribution in the walls, patients may suffer from pathologies inducing heterogeneities in RA or LA uptake. However, RR methods tend to reconcentrate the detected activity in the regions where it originates. If heterogeneities larger than the spatial resolution of the PET system are located in the RA or LA walls, they will still be visible after RR.

One limitation of the present study is that there was no patient motion compensation for breathing and cardiac motions. The heart motion impact on the present results is difficult to evaluate. Using cardiac gating acquisition would help the quantification with the RR method applied on each gated bin separately, and afterward summing together the activities of the bins to recover the non-gated statistics. Without gating the RA and LA walls on the PET image are enlarged by the heart motion. The RR cannot correct for that motion but it will still recover the activity in that enlarged wall, improving the quantification as in that case the VOIs will have to be enlarged too to take the motion blurring into account. The same analysis holds in the case of atrial fibrillation and enlargement.

As the reconstruction algorithms with RR, seen as black boxes by the end user, might strongly differ between manufacturers, the optimized parameters found in this study are only adapted to the Philips Vereos TOF-PET/CT, that is, still state-of-the-art system with its 310 ps TOF FWHM. The observed trends for the activity recovery and for the SNR convergences would probably be similar for other systems but this needs to be checked per TOF-PET/CT system in order to extract the best set of reconstruction parameters.

Conclusions

The Philips Vereos TOF-PET/CT images reconstructed with the manufacturer four iterations/15 subsets OSEM algorithm including a PSF RR with five iterations/six regularization can be used to quantitatively evaluate the left atrium uptake in ^{18}F-FDG cardiac studies while still preserving image reading quality. This may lead to a more precise evaluation of the metabolic cardiac status of cardiovascular disease, especially when the atria are concerned.

Acknowledgements

Sébastien Marchandise received funding from a Daiichi Sankyo grant.

Posted history: This article was previously posted to ResearchSquare: doi: https://doi.org/10.21203/rs.3.rs-1719799/v1.

Ethics approval and consent to participate: All patients provided written informed consent. The TRIATLON study was approved by the Institutional Ethics Committee of Brussels Cliniques Universitaires Saint-Luc.

All methods were carried out in accordance with the ethical standards as laid down in the 1964 Declaration of Helsinki and its later amendments or comparable ethical standards.

Conflicts of interest

There are no conflicts of interest.

References

1 Thomas L, Abhayaratna W. Left atrial reverse remodeling. Mechanisms, evaluation, and clinical significance. *J Am Coll Cardiol Img* 2017; **10**:65–77.

2 Alfuhied A, Kanagala P, McCann G, *et al*. Multi-modility assessment and role of left atrial function as an imaging biomarker in cardiovascular disease. *Int J Cardiovasc Imaging* 2021; **37**:3355–3369.

3 Olsen FJ, Bertelsen L, de Knegt MC, Christensen TE, Vejlstrup N, Svendsen JH, *et al*. Multimodality cardiac imaging for the assessment of left atrial function and the association with atrial arrythmias. *Circ Cardiovasc Imaging* 2016; **9**:e004947.

4 Ghezelbash S, Molina CE, Dobrev D. Altered atrial metabolism: an underappreciated contributor to the initiation and progression of atrial fibrillation. *J Am Heart Assoc* 2015; **4**:e001808.

5 Yodogawa K, Fukushima Y, Ando T, Iwasaki YK, Akiyama K, Kumita SI, *et al*. Prevalence of atrial FDG uptake and association with atrial arrhythmias in patients with cardiac sarcoidosis. *Int J Cardiol* 2020; **313**:55–59.

6 Rennison JH, Li L, Lin CR, Lovano BS, Castel L, Wass SY, *et al*. Atrial fibrillation rhythm is associated with marked changes in metabolic and myofibrillar protein expression in left atrial appendage. *E J Physiol* 2021; **473**:461–475.

7 Lange PS, Avramovic N, Frommeyer G, Wasmer K, Pott C, Eckardt L, *et al*. Routine 18F-FDG PET/CT does not detect inflammation in the left atrium in patients with atrial fibrillation. *Int J Cardiovasc Imaging* 2017; **33**:1271–1276.

8 Xie B, Chen BX, Wu JY, Liu X, Yang M-F. Factors relevant to atrial 18F-fluorodeoxyglucose uptake in atrial fibrillation. *J Nucl Cardiol* 2020; **27**:1501–1512.

9 Surti S, Kuhn A, Werner ME, Perkins AE, Kolthammer J, Karp JS. Performance of Philips Gemini TF PET/CT scanner with special considerations for its time-of-flight imaging capabilities. *J Nuc Med* 2007; **48**:471–480.

10 Zhang J, Maniawski P, Knopp MV. Performance evaluation of the next generation solid-state digital photon counting PET/CT system. *EJNMMI Res* 2018; **8**:97.

11 Rausch I, Ruiz A, Valverde-Pascual I, Cal-González J, Beyer T, Carrio I. Performance evaluation of the Vereos PET/CT system according to the NEMA NU2-2012 standard. *J Nucl Med* 2019; **60**:561–567.

12 Reddin S, Scheuermann JS, Bharkhada D, Smith AM, Casey ME, Conti M, Karp JS. Performance evaluation of the SiPM-based siemens biograph vision PET/CT system. *IEEE Nucl Sci Symp Med Imaging Conf Proc (NSS/MIC)* 2018; **1**:1–5. doi: 10.1109/NSSMIC.2018.8824710.

13 Zhang B, Olivier P, Lorman B, Tung CH. PET image resolution recovery using PSF-based ML-EM deconvolution with blob-based list-mode TOF reconstruction. *J Nucl Med* 2011; **52**(Supplement 1):266.

14 Rasband WS. ImageJ, U. S. National Institutes of Health. Bethesda, Maryland, USA, 1997-2018. https://imagej.nih.gov/ij/. [Accessed 24 March 2023]

15 Sage D, Donati L, Soulez F, Fortun D, Schmit G, Seitz A, *et al*. DeconvolutionLab2: an open-source software for deconvolution microscopy. *Methods-Image Process Biol* 2017; **115**:28–41.

16 Bertero M, Boccacci P. *Introduction to inverse problems in imaging*. CRC press; 2020.

17 Tsutsui Y, Awamoto S, Himuro K, Umezu Y, Baba S, Sasaki M. Edge Artifacts in point spread function-based PET reconstruction in relation to object size and reconstruction parameters. *Asia Ocean J Nucl Med Biol* 2017; **5**:134–143.

18 Munk OL, Tolbod LP, Hansen SB, Bogsrud T. Point-spread function reconstructed PET images of sub-centimeter lesions are not quantitative. *EJNMMI Phys* 2017; **4**:5–17.